Review TRENDS in Biotechnology Vol.25 No.4

Nanopore sequencing technology: nanopore preparations

Minsoung Rhee[1] and Mark A. Burns[1,2]

[1] Department of Chemical Engineering, University of Michigan Ann Arbor, MI 48109, USA
[2] Department of Biomedical Engineering, University of Michigan Ann Arbor, MI 48109, USA

For the past decade, nanometer-scale pores have been developed as a powerful technique for sensing biological macromolecules. Various potential applications using these nanopores have been reported at the proof-of-principle stage, with the eventual aim of using them as an alternative to *de novo* DNA sequencing. Currently, there have been two general approaches to prepare nanopores for nucleic acid analysis: organic nanopores, such as α-hemolysin pores, are commonly used for DNA analysis, whereas synthetic solid-state nanopores have also been developed using various conventional and non-conventional fabrication techniques. In particular, synthetic nanopores with pore sizes smaller than the α-hemolysin pores have been prepared, primarily by electron-beam-assisted techniques: these are more robust and have better dimensional adjustability. This review will examine current methods of nanopore preparation, ranging from organic pore preparations to recent developments in synthetic nanopore fabrications.

Introduction

Nanometer-scale pores have been widely investigated for various applications in nanobiotechnology [1,2]. In particular, researchers have applied nanopores as stochastic sensors for biological molecules. These sensors can identify and quantify analytes based on the conductance of current through the pore [3–5]. Given that the scale of such nanopores is comparable with the macromolecules of interest, molecules entering the pore can be easily monitored and analyzed individually. For example, the diameter of stretched single-stranded DNA (ssDNA) is ~1.3 nm, whereas the diameter of α-hemolysin nanopores is 1.5 nm [6]. Thus, the ssDNA is straightened from its randomly coiled state as it passes through the pore, making nanopores attractive for *de novo* DNA sequencing because they enable nucleotides to be examined in a serial manner.

The principle underlying such nanopore sensors is straightforward. Nanopores can act as Coulter counters [7], in which molecules carrying a net electrical charge are electrophoretically driven through the pore by an applied electric potential; they then physically block the pore, which produces measurable changes in ionic conductivity [8]. This analytical technique has proven effective in determining the concentration and size distribution of particles down to the sub-micrometer level [4]. Various nanopore applications have adopted and extended the Coulter counter concept from the simple counting of molecules passing by to analyzing the resultant electrical signals for further information such as base discrimination. The general uses of such nanopores are summarized in Box 1. A more detailed review on nanopore modifications and applications is available elsewhere [2].

To date, there have been two general approaches to prepare nanopores for DNA analysis. The first approach uses well-known organic membrane proteins such as α-hemolysin [8]. The α-hemolysin pore has been particularly well explored and even modified to the specific needs of various analytes [5], mainly because of its ideal pore size, low level of noise and well-established preparation protocol [1,9]. In addition to α-hemolysin, other membrane-bound proteins of various sizes and functionalities have also been investigated [10–13]. Although the majority of nanopore DNA analysis to date has been performed with organic nanopores, various synthetic nanopores have been developed, independently, using conventional or non-conventional fabrication techniques [14–18].

This review will present current nanopore technologies, ranging from organic pore preparations to recent developments in synthetic nanopore fabrications. A more thorough overview of the organic pore and its applications can be found in excellent review articles by Nakane *et al.* [1] and Schmidt [3]

Protein nanopore preparation

The α-hemolysin pore

The first attempts to produce nanopores to detect single DNA polynucleotides were made with α-hemolysin, a transmembrane protein, inserted in a lipid bilayer [8,19]. α-Hemolysin is a monomeric, 33 kD, 293 residue protein that is secreted by the human pathogen *Staphylococcus aureus*. These monomers self-assemble as a heptamer on synthetic lipid bilayers to form a 1.5 nm diameter aqueous channel through the membrane [6]. Kasianowicz *et al.* found that the α-hemolysin pore remains open at neutral pH and high ionic strength [8]. Furthermore, the α-hemolysin pore passes a steady ionic current in a detectable range, whereas most membrane channels exhibit unstable current levels due to their high sensitivity and spontaneous gating. This steady current flow across a relatively large range ensures a low level of background electrical noise and thus prevents the electrical signals of interest from being masked. Crystallography has revealed

Corresponding author: Burns, M.A. (MABurns@UMich.edu).
Available online 22 February 2007.

 0167-7799/$ – see front matter doi:10.1016/j.tibtech.2007.02.008

Box 1. A summary of the recent uses of nanopores in nucleic acid analyses [2]

Molecular discrimination

(i) Discrimination between ssDNA and dsDNA: the inherent structure of α-hemolysin nanopores is ideal for discriminating ssDNA from dsDNA because of the pore size (1.5 nm) [6,8,16].
(ii) Discrimination among homopolymeric RNA and/or DNA molecules: the blockade patterns of the different homopolymeric RNA and/or DNA molecules can be statistically distinguished from one another using current blockade amplitude and translocation duration [19,64].
(iii) Assessment of nucleic acid preparation: the level of breakdown of a sample is measurable by comparing the nanopore translocation profile of freshly prepared sample and the same molecule after storage, dephosphorylation, phosphorylation or other manipulations [65].
(iv) DNA strand length discrimination: it has been observed that the number of blockades produced by short DNA molecules per unit time is significantly greater than the number produced by equivalent concentrations of longer molecules [8] – the longer a DNA strand is, the longer it takes to negotiate the pore [14].

Modifications of nanopore detection

(i) Discrimination among individual DNA hairpin molecules: DNA hairpins are used instead of ssDNA to increase the translocation duration of a single molecule of DNA in the α-hemolysin channel at relatively long (milliseconds to seconds) intervals [66].
(ii) Detection of complementary polynucleotides from engineered nanopores: with a covalently tethered DNA molecule near the entrance of the α-hemolysin pore, the biosensor can distinguish a single base mismatch [9,67].
(iii) Translocation of modified analyte polynucleotides: covalently linked dumbbell-shaped DNA–polymer complexes are used as analytes to increase translocation duration for improved resolution [68,69].
(iv) Translocation of single nucleotides: individual nucleotides are modified by attaching an interactive adaptor and fed through the nanopore sensor [70].
(v) Investigation of ionic currents through synthetic nanopores during DNA translocations as a function of the ionic concentration and the applied electric field [50,71].

the structure of the α-hemolysin pore to 1.9 Å resolution [6]. The resulting image shows a 100 Å-long, mushroom-shaped, homo-oligomeric heptamer, of which the pore has a limiting aperture of 1.5 nm (Figure 1a). The transmembrane domain of the channel comprises a 14-strand beta barrel, which is primarily hydrophilic inside and hydrophobic outside.

To produce a nanopore, α-hemolysin subunits are introduced into a buffered solution that is in contact with a planar lipid bilayer, separated in solution into two compartments (designated *cis* and *trans*): the head of the α-hemolysin molecule is frequently referred to as the *cis* side, and the stem end as the *trans* side. The assembled heptameric complex inserts into the *cis* side of the bilayer to produce a pore that can carry an ionic current of approximately 120 pA (picoAmperes), with an applied voltage of 120 mV. The lipid bilayer containing the nanopore also influences its function as an ion channel. Such bilayers are suited for single-channel recording of ionic current and can also be incorporated onto a silicon chip for miniaturization and automated operation [20,21].

Other organic pores

Beyond α-hemolysin, the use of other membrane-bound proteins with appropriate structures and properties has also been investigated. Such proteins have been isolated and assembled into artificial lipid bilayers for DNA analysis based on DNA translocation. The voltage-dependent mitochondrial ion channel (VDAC), or mitochondrial porin, is a highly conserved, monomeric protein located in the mitochondrial outer membrane [22]. Each VDAC channel, consisting of a single 30 kDa polypeptide, forms an aqueous pore ~3 nm in diameter [23]. This differs from the α-hemolysin pore because the pore size is large enough for double-stranded DNA to translocate through it. VDAC pores are produced in a planar lipid bilayer, using a technique similar to that of the α-hemolysin method [10].

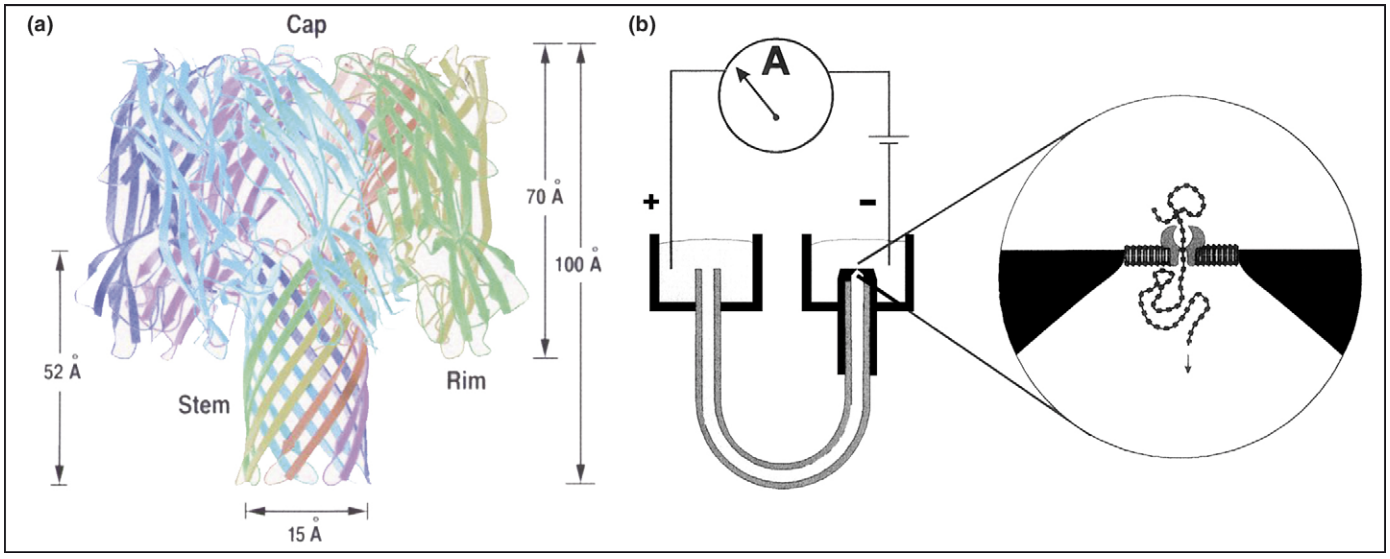

Figure 1. **(a)** Ribbon representation of the α-hemolysin heptamer; each color represents a different promoter [6]. **(b)** An early prototype nanopore device. A U-shaped tube connects two reservoirs filled with ion buffer (left). The reservoirs are connected to an ammeter by Ag–AgCl electrodes, and nucleic acids are driven through the α-hemolysin pore by an applied voltage (right) [19].

Bacterial pore proteins are often considered as promising alternatives to α-hemolysin. The bacterial ion channels from the membrane vesicles of *Bacillus subtilis* have been incorporated into phospholipid bilayers. These ion channels were found to be large enough to translocate 4.2 kb, double-stranded plasmids [11], with a measurable reduction of the ionic current. The translocation was verified by standard PCR of the *trans*-chamber solution. Similarly, OmpF porins from the outer membranes of *E. Coli* have been also investigated with regard to the transport process [12,13,24] – OmpF channels comprise homotrimeric units when reconstituted into planar lipid bilayers. An OmpF pore diameter of 1.0–1.2 nm, which might be large enough for the translocation of single-stranded DNA strands, was proposed [13]. Although initial work with OmpF has reported the detection of water-soluble polymers, such as poly(ethylene glycol)s [12], detection of DNA molecules moving through the pore has not yet been reported [3].

For single-stranded DNA analyses, the use of a nucleic acid binding and/or channel protein (NAC) has been proposed [25,26]. Hanss *et al.* identified a 45 kDa protein purified from rat renal brush border membrane (BBM) that binds oligonucleotide sequences [25]. When a single NAC is incorporated into an artificial lipid membrane, the presence of oligonucleotides is indispensable for channel activity: the addition of oligonucleotides to the solution activates the gate opening process and yields a detectable current rise, with explicit transitions between the closed and open state of the channel. Another application of nanopores for analyte detection includes the use of gramicidin pores, which are mini-proteins, composed of two tryptophan-rich subunits. Wright-Lucas and Harding modified gramicidin pores by adding streptavidin-binding sites and attaching biotinylated oligonucleotide probes [27]. Given that gramicidin pores are not large enough to even translocate ssDNA directly, a different detection scheme has been adopted that uses tethered probe molecules. When the sequence between the target and the probe matches perfectly, the ionic current through the gramicidin pores suddenly vanishes, acting as a switch biosensor. Based on this detection mechanism, real-time measurement of the reaction rates of oligonucleotide hybridization has been performed [27].

The reasons to investigate proteins other than α-hemolysin are not limited to seeking organic pores of varying sizes. It is probable that other proteins can be prepared with less laborious procedures and can be used with less modification. Furthermore, other proteins might exhibit a simpler structure, be more robust and have better reproducibility [3] Box 2.

Box 2. Take-home messages

– Most DNA analyses, to date, have been performed using α-hemolysin protein pores owing to their ideal characteristics for the detection and identification of ssDNA.
– In the near future, it is probable that synthetic nanopores will replace the α-hemolysin protein pores as fabrication techniques for synthetic nanopores become more reliable and reproducible.
– The use of synthetic pores will enable fully integrated nanopore microfabricated systems, as a major step toward cheap *de novo* sequencing.

Synthetic nanopore fabrications

Protein nanopores have been used as functioning electronic sensors to identify single molecules. However, in lipid bilayers, these nanopores have size, variation and stability limitations: proteins are usually labile; the lipid membranes are fragile; the pore diameter is fixed; and the range of safe electrical operation is narrow [15,16,28]. Although α-hemolysin self-assembles with high fidelity and reproducibility, the physical, chemical and electrical properties of this protein nanopore pose limitations on the experimental possibilities. For example, the high temperatures and/or strong denaturants required to maintain polynucleotides in a single-stranded state can disrupt the fragile α-hemolysin protein–lipid assembly [17]. In addition, a detailed understanding of the signals obtained empirically has been complicated by the complex charge distribution of the channel. Moreover, considering that a passing molecule is present throughout the 5 nm-long pore [6], the conductance changes reflect the sum of up to 10–15 nucleotides covering the length of the pore. This duplicated occupation of the pore by multiple nucleotides hinders single-nucleotide resolution through changes in electrical signals.

To overcome these difficulties, solid-state synthetic nanopores are being fabricated using various means [28]. The surface properties of a nanopore must be carefully selected to respond sensitively to the molecules that are to be detected [29]. Present state-of-the-art semiconductor fabrication techniques using photolithography are limited to feature sizes of the order of tens of nanometers [1], which is larger than would be typically required for the detection of individual DNA molecules using the Coulter counter effect. To achieve much smaller feature sizes on the scale required for detection of biomolecules, other specialized fabrication techniques must be applied. These techniques are presented in the following sub-sections and summarized in Table 1.

Ion beam sculpting

Massive ions with energies of several thousand electron volts (eV) cause nanometer-scale atomic rearrangements when fired at the surface of materials. When an ion beam impacts the surface of a material, an erosion process called sputtering occurs as the ion beam removes atoms from the outermost layers. Li *et al.* prepared a flat Si_3N_4 surface containing a bowl-shaped cavity on one side, and impinged on the opposite surface with argon ion beams [30] (Figure 2a). As material is removed from the flat Si_3N_4 surface, the surface will ultimately intercept the bottom of the cavity, which causes a pore to open. By implementing a feedback-controlled ion sputtering system, they could extinguish the erosion process upon breakthrough and thus create a molecular-scale pore as small as 1.8 nm (Figure 2b). This feedback-controlled system also controls other important parameters, including sample temperature, beam cycle and ion beam flux [31,32].

Although a nanopore can be created from a cavity in the membrane under conditions where the sputtering erosion

Table 1. Nanopores from various preparation procedures

	Protein α-Hemolysin assembly	Synthetic Ion beam sculpting	Micro-molding	Latent track etching	E-beam fine tuning	Nanotubes
Minimum pore diameter reported (nm)	1.5 (fixed)	1.8	80	2.0	1.0	50
Membrane material	Lipid bilayer	Si_3N_4	PDMS	Poly-carbonate	Si, SiO_2, Si_3N_4	Epoxy, Si_3N_4
Pore material	α-hemolysin	Si_3N_4, Al_2O_3		Gold layer		MWNT
Remarks	Mass production	Size tuning	Easy fabrication	Conical shape	Visual fine tuning	Stable, uncharged

process dominates, the ion beam can also be used to stimulate the lateral transport of matter, which causes a pre-existing larger pore, such as a focused ion beam (FIB) drilled pore, to close [33–35]. At room temperature, the transmitted ion-counting rate decreases with increasing ion beam exposure. By changing the sample temperature or ion beam parameters during the process, it is possible to control whether pore opening or closing dominates. At temperatures <5°C the sputtering process dominates, whereas at >5°C the lateral mass transport process dominates. This ion-beam-induced pore-closing phenomenon was closely monitored by Mitsui *et al.*, and it is argued that matter accretion might be influenced by the surface electric field and the geometry of the pore wall [36].

Schenkel *et al.* fabricated an ~4 nm-wide hole in a silicon nitride membrane using a dual-beam focused ion beam system [18]. Low stress silicon nitride membranes on silicon frames were coated with a thin gold or gold/palladium layer to minimize charging effects during exposure to ion beams. Initially, a high intensity gallium ion beam was used to drill holes from 50 to 600 nm in diameter. The ion beam was further used to deposit a thin platinum film to close the hole slowly. Similarly, Lo *et al.* recently manufactured nanopores with diameters smaller than 5 nm using the ion beam sculpting technique; however, they used a commercial FIB system equipped with a scanning electron microscope (SEM), which enables a convenient visual feedback control during the size-tuning process [37].

Chen *et al.* suggested that atomic layer deposition (ALD) can afford a finishing step, to fine tune the sizes of nanopores fabricated by ion beam sculpting [29]. ALD from the vapor phase was proved to be highly conformal [38,39] – providing a uniform coating to all exposed surfaces – and because layers are deposited inside the pore, the pore maintains its initial shape and only reduces its size. Because of this uniform and incremental ALD, the sidewalls lining the diameter of a nanopore can be fashioned with atomic precision, shrinking an oversized pore to a preferred smaller diameter. Using this technique, nanopores with various diameters were easily produced, based upon the calibrated deposition rate of 0.099 ± 0.012 nm per reaction cycle [29]. Depending on the choice of the coating material, ALD also adjusts the surface properties of nanopores. Aluminum oxide can be used as the coating material to overcome not only electrostatic repulsion inside the pore but also any electro osmotic flow caused by the sidewalls [29]. Moreover, Al_2O_3 is a thermally and chemically stable, insulating, dielectric material that inhibits direct electron tunneling.

Micromolding

Saleh and Sohn reported a fundamentally different artificial nanopore that can be fabricated using micromolding

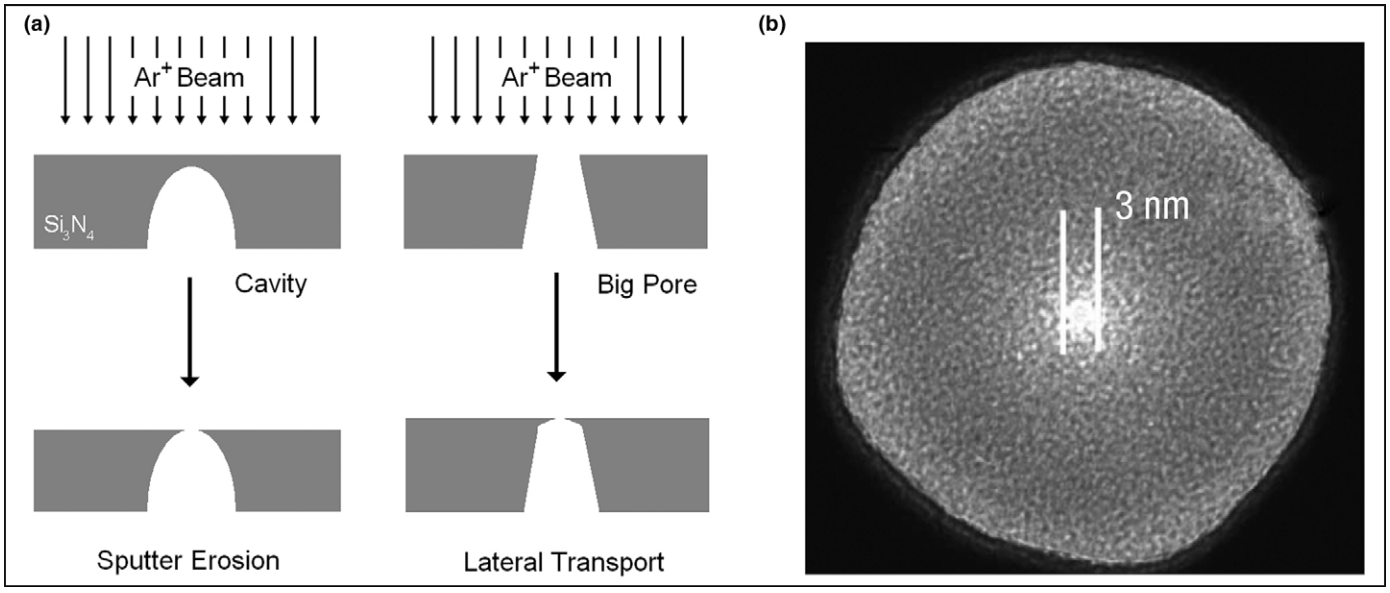

Figure 2. **(a)** Ion bean sculpting to make nanopores from a cavity (left) or from a through hole (right). Either sputter erosion or lateral transport processes dominate, depending on the selected conditions used in the ion beam sculpting apparatus [30]. **(b)** TEM image of a 3 nm silicon nitride nanopore produced by ion beam sculpting [14]. Pores as small as 1.8 nm have been created.

techniques [40,41]. The pore is 3 μm in length, has a diameter of 200 nm and connects two large electrolyte reservoirs. Conventional lithographic techniques are used to create a negative master of the pore and reservoirs, which is subsequently cast into a poly(dimethylsiloxane) (PDMS) slab. The master is produced in two steps: first, electron-beam lithography is used to pattern a 200 nm-wide, 200 nm-thick polystyrene line on a silicon substrate, forming the negative of the pore; next, photolithography is used to create the negatives of the reservoirs. The durability of both the polystyrene and SU-8 photoresists enables the repeated use of the master. The created master is then cast into a slab of PDMS, and electrodes are patterned onto a glass slip anchored by metal deposition. These steps lead to the creation of much larger channels that serve as detectors for large molecules.

The minimum achievable pore diameter with PDMS was reported to be as small as 80 nm, in the recent work by Schmid and Michel [42]. Regardless of its relatively large minimal feature size, the ease and simplicity of micromolding meaningfully enhances the capabilities of various synthetic nanopores for molecular sensing, particularly for the coarse sizing of large DNA molecules. Moreover, this approach enables the rapid and reproducible fabrication of submicrometer-scale pores and is easy to modify structurally and chemically for various detection applications. Note that arrays of pores can be created by this technique for the simultaneous measurement of many different molecules.

Latent track etching

In recent studies, a single conical nanopore was created in a polymer substrate by chemically etching the latent track of a single, energetic, heavy ion [43,44]. Fabrication of the nanopore by the track-etching technique is based on irradiation of a polymer film with nuclear fragments of a total kinetic energy ranging from hundreds to thousands of mega electron volts (MeV), and the subsequent chemical etching of the latent ion tracks. Each ion produces an etchable track in a polymer foil, forming a one-pore membrane [45]. The size and axial uniformity of the pore can be customized with nanometer precision by controlling the type and concentration of the etchant, the temperature, and the etching duration. To obtain a conical shape, foil was placed between two chambers and etched from one side; the other chamber was filled with a neutralizing medium. The etching stops when an increase in the current is detected, indicating the moment of break-through between the chambers. To form a low density of pores, the flux of nuclear fragments must be controlled at the membrane surface, enabling localization of individual tracks by limiting the contact area of the electrolyte to the membrane. Alternatively, by relying on common microfabrication techniques, a single pore can be isolated by physically blocking all other pores with an epoxy coating or a tape mask [46].

Smaller pore diameters and lengths can be attained by using track-etched polycarbonate membranes as templates for gold nanotubules. The nanotubules are formed by plating in gold solution using a chemical reduction process that deposits gold without the use of an externally applied electric potential [47]. This technique coats the pore walls and membrane faces with a thin (a few nm) layer of gold, decreasing the size of the pore opening to 2 nm.

Electron beam-induced fine tuning

Recently, nanopores in various materials were fabricated by advanced nanofabrication techniques, such as FIB drilling and electron (E)-beam lithography, followed by E-beam-assisted fine-tuning techniques [16,32,48]. Since Storm *et al.* pioneered the use of high-energy electron beams to fine tune the size of silicon oxide nanopores [48], it has become one of the most popular methodologies to fabricate small nanopores [37,49–54]. As a starting material, silicon-on-insulator (SOI) wafers, with a top single-crystal silicon layer 340 nm thick, were used to fabricate free-standing silicon membranes [48]. A thermal oxidization process was then used to produce a 40 nm-thick SiO_2 layer on both sides of the membranes: first, squares were opened in the top SiO_2 mask layer using electron-beam lithography and reactive-ion etching; subsequently, pyramid-shaped holes were etched using anisotropic KOH wet etching; finally, the holes were thermally oxidized to form a SiO_2 surface layer with a thickness of 40 nm (Figure 3).

To fine tune the size of pores at nanometer precision, Storm *et al*. used a commercial transmission electron

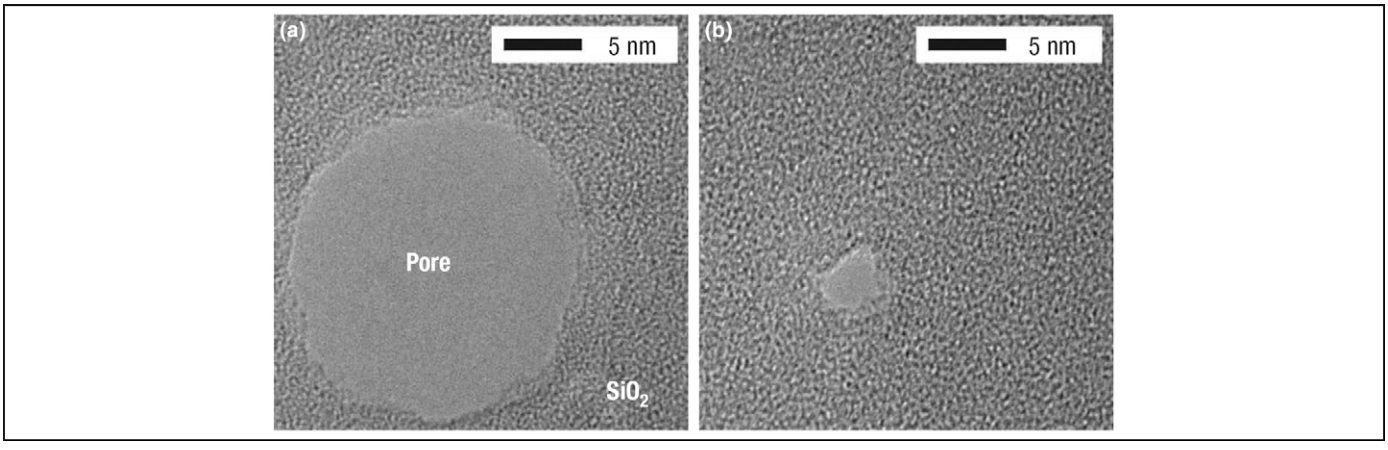

Figure 3. TEM images of a silicon oxide nanopore. **(a)** The starting size and **(b)** the final size during imaging in a TEM microscope. The electron irradiation causes a 6 nm pore to shrink gradually down to a size of ~2 nm [48].

microscope (TEM) operated at a voltage of 300 kV. The high electron intensity deforms the material surface, modifying the dimensions of the silicon oxide nanopores in a controlled way. With appropriate electron beam intensity and initial diameter, pores tend to shrink. The change in pore diameter is monitored in real-time using the imaging mechanism of the microscope, providing a feedback mechanism to switch off the electron beam so that the material can quench and retain its shape. It was reported that the diameter of the pore shrinks at a rate of ~0.3 nm per minute, which is slow enough to stop at any desired dimension [48].

Keyser *et al.* and Heng *et al.,* independently, adopted a similar strategy to fabricate nanopores in ultra-thin membranes [16,32,49,51]. Heng *et al.* produced, with subnanometer precision, 1 nm-diameter pores in robust metal oxide semiconductor (MOS)-compatible membranes by using a tightly focused, high-energy electron beam from TEM. Likewise, conventional semiconductor microfabrication techniques enabled Ho *et al.* to form robust Si, SiO_2, and Si_3N_4 free-standing membranes that could withstand hundreds of electrolyte immersion and emersion cycles without failing [52]. Successive, tightly focused TEM operations resulted in membrane surface decomposition and sputtering; thus creating a single nanopore in the membrane. Likewise, Keyser *et al.* produced a 4 nm nanopore in 20 nm, low-stress silicon nitride membranes [49].

Based on the concept of E-beam fine tuning, there have been different approaches in achieving the final pore dimension. Chang *et al.* used a field emission scanning electron microscope (FESEM) as an electron beam source, and reported different pore shrinking behavior [54]: they found that pore shrinkage from a FESEM E-beam was independent of the initial pore size, and pore enlargement did not occur. By contrast, Lo *et al.* suggested a combinational method of ion beam sculpting and E-beam fine-tuning: they first reduced the diameter of SiN nanopores to ≤10 nm, and then applied a TEM fine-tuning technique to further shrink the pore to 1 nm [37].

This lithography strategy to produce synthetic pores in ultra-thin membranes has obvious superiorities compared with ion-beam sculpting [30] or ion-track etching [43] because of the tight focus and high flux of the electron beam. Direct visual feedback for fine tuning and the use of a wide variety of membrane materials are additional advantages [53]. However, despite the extensive use of this technique, the understanding of atomic flow on the surface induced by E-beam impingement is limited [55]. Storm *et al.* performed a set of TEM-tuning experiments with their silicon oxide nanopores, and concluded that the shrinking process was driven by surface tension minimization [56]. They also suggested that the electron beam breaks chemical bonds at low temperatures, and the surface changes into a glass-like material, which eventually flows and deforms. Nevertheless, to assure the reproducible control of pore tuning on various materials, the underlying physics must be further explored.

Inorganic nanotubes

Instead of fabricating silicon-based nanopores, Crooks and his collaborators showed that carbon nanotubes might also be suitable for Coulter counting [57]. Figure 4 illustrates the proposed procedures to prepare single-channel membranes through the embedding of multiwall carbon nanotubes (MWNTs). They first sealed a stretched, single MWNT within liquid epoxy; after polymerization, the polymeric monolith containing the MWNT was sectioned using a microtome. The resulting fabricated nanotube channels ranged from 50–160 nm in diameter [58,59].

There are several advantages to using carbon nanotubes compared with other synthetic nanopores. First, carbon nanotubes have uniform and well-defined chemical and structural properties compared with nanopores treated by high-energy beams [60]. Second, various sized nanotubes can be obtained, ranging from one to hundreds of nanometers; thus, it is easier to tailor the channel size to the potential analytes. Third, the surface charge of the MWNT channel is known to be, effectively, zero [61]; therefore,

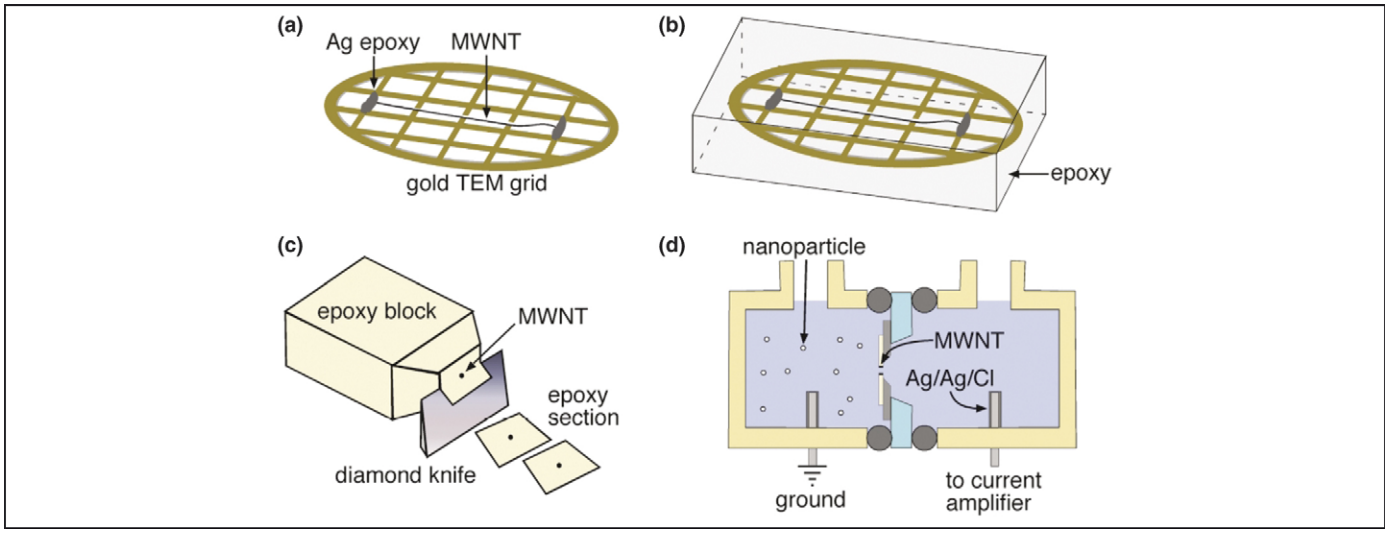

Figure 4. Illustration of the method for the fabrication of MWNT membranes. **(a)** The extracted nanotube is stretched and fixed to a TEM grid; **(b)** the MWNT-containing grid is encased within a liquid epoxy; **(c)** the resulting monolith is sectioned from the epoxy block; and **(d)** a support structure immobilizes the membrane and separates the two chambers [59].

electrophoretic transport becomes simple enough so that the electrically driven mobility of particles can be predicted without complicated assumptions.

Recently, Fan *et al.* fabricated silica nanotubes directly integrated with microfluidic systems, to form a nanoparticle-sensing device [62]. After silicon nanowires were synthesized by $SiCl_4$ chemical vapor deposition, the wires were translated into silica nanotubes through an oxidation and etching process, and controlled pore sizes down to 10 nm were obtained. Such nanotubes present their unique aspect ratio and provide a new platform for Coulter counter as well as the potential for easy integration into nanofluidic circuits.

Conclusion

Despite the continuing developments in synthetic nanopore fabrication, the majority of DNA analyses to date have been performed using α-hemolysin protein pores, partly because α-hemolysin pores have almost ideal characteristics for the detection and identification of ssDNA. However, when considering the technical achievements to date, it is unlikely that synthetic nanopores will replace their biological counterparts in the near future because of the underlying complications with synthetic nanopores, for example, atomic flow phenomena needs to be investigated and clarified. Furthermore, the use of synthetic pores will enable fully integrated microfabricated systems based on nanopore detection [63] and, thus, will accelerate steps toward *de novo* sequencing.

References

1 Nakane, J.J. *et al.* (2003) Nanopore sensors for nucleic acid analysis. *J. Phys. Condens. Matter* 15, R1365–R1393
2 Rhee, M. and Burns, M.A. (2006) Nanopore sequencing technology: research trends and applications. *Trends Biotechnol.* 24, 580–586
3 Schmidt, J. (2005) Stochastic sensors. *J. Mater. Chem.* 15, 831–840
4 Bezrukov, S.M. (2000) Ion channels as molecular Coulters to probe metabolite transport. *J. Membr. Biol.* 174, 1–13
5 Bayley, H. and Cremer, P.S. (2001) Stochastic sensors inspired by biology. *Nature* 413, 226–230
6 Song, L. *et al.* (1996) Structure of staphylococcal alpha-hemolysin, a heptameric transmembrane pore. *Science* 274, 1859–1865
7 DeBlois, R.W. and Bean, C.P. (1970) Counting and sizing of submicron particles by resistive pulse technique. *Rev. Sci. Instrum.* 41, 909–916
8 Kasianowicz, J.J. *et al.* (1996) Characterization of individual polynucleotide molecules using a membrane channel. *Proc. Natl. Acad. Sci. U. S. A.* 93, 13770–13773
9 Winters-Hilt, S. (2006) Nanopore detector-based analysis of single-molecule conformational kinetics and binding interactions. *BMC Bioinformatics* 7 (Suppl. 2), S21
10 Szabo, I. *et al.* (1998) Double-stranded DNA can be translocated across a planar membrane containing purified mitochondrial porin. *FASEB J* 12, 495–502
11 Szabo, I. *et al.* (1997) DNA translocation across planar bilayers containing *Bacillus subtilis* ion channels. *J. Biol. Chem.* 272, 25275–25282
12 Rostovtseva, T.K. *et al.* (2002) Partitioning of differently sized poly(ethylene glycol)s into OmpF porin. *Biophys. J.* 82, 160–169
13 Nestorovich, E.M. *et al.* (2003) Residue ionization and ion transport through OmpF channels. *Biophys. J.* 85, 3718–3729
14 Li, J. *et al.* (2003) DNA molecules and configurations in a solid-state nanopore microscope. *Nat. Mater.* 2, 611–615
15 Wang, H. and Branton, D. (2001) Nanopores with a spark for single-molecule detection. *Nat. Biotechnol.* 19, 622–623
16 Heng, J.B. *et al.* (2004) Sizing DNA using a nanometer-diameter pore. *Biophys. J.* 87, 2905–2911
17 Chen, P. *et al.* (2004) Probing single DNA molecule transport using fabricated nanopores. *Nano Lett.* 4, 2293–2298
18 Schenkel, T. *et al.* (2003) Formation of a few nanometer-wide holes in membranes with a dual-beam focused ion beam system. *J. Vac. Sci. Technol. B* 21, 2720–2723
19 Akeson, M. *et al.* (1999) Microsecond time-scale discrimination among polycytidylic acid, polyadenylic acid, and polyuridylic acid as homopolymers or as segments within single RNA molecules. *Biophys. J.* 77, 3227–3233
20 Mayer, M. *et al.* (2003) Functional analysis of ion channels: planar patch clamp and impedance spectroscopy of tethered lipid membranes, In *Biosensors – A Practical Approach*, (2nd edn), Oxford University Press
21 Mayer, M. *et al.* (2003) Microfabricated teflon membranes for low-noise recordings of ion channels in planar lipid bilayers. *Biophys. J.* 85, 2684–2695
22 Rostovtseva, T.K. *et al.* (2002) Dynamics of nucleotides in VDAC channels: structure-specific noise generation. *Biophys. J.* 82, 193–205
23 Song, J. *et al.* (1998) The topology of VDAC as probed by biotin modification. *J. Biol. Chem.* 273, 24406–24413
24 Danelon, C. *et al.* (2004) Channel-forming membrane proteins as molecular sensors. *IEEE Trans. Nanobioscience* 3, 46–48
25 Hanss, B. *et al.* (1998) Identification and characterization of a cell membrane nucleic acid channel. *Proc. Natl. Acad. Sci. U. S. A.* 95, 1921–1926
26 Leal-Pinto, E. *et al.* (2005) Presence of the nucleic acid channel in renal brush-border membranes: allosteric modulation by extracellular calcium. *Am. J. Physiol. Renal Physiol.* 289, F97–F106
27 Wright-Lucas, S. and Harding, M.M. (2000) Detection of DNA via an ion channel switch biosensor. *Anal. Biochem.* 282, 70–79
28 Deamer, D.W. and Branton, D. (2002) Characterization of nucleic acids by nanopore analysis. *Acc. Chem. Res.* 35, 817–825
29 Chen, P. *et al.* (2004) Atomic layer deposition to fine tune the surface properties and diameters of fabricated nanopores. *Nano Lett.* 4, 1333–1337
30 Li, J. *et al.* (2001) Ion-beam sculpting at nanometer length scales. *Nature* 412, 166–169
31 Stein, D. *et al.* (2004) Feedback-controlled ion beam sculpting apparatus. *Rev. Sci. Instrum.* 75, 900–905
32 Heng, J.B. *et al.* (2005) Stretching DNA using the electric field in a synthetic nanopore. *Nano Lett.* 5, 1883–1888
33 Stein, D. *et al.* (2002) Ion-beam sculpting time scales. *Phys. Rev. Lett.* 89, 27–30
34 Brongersma, M.L. *et al.* (2000) Origin of MeV ion irradiation-induced stress changes in SiO_2. *J. Appl. Phys.* 88, 59–64
35 Fologea, D. *et al.* (2005) Detecting single-stranded DNA with a solid state nanopore. *Nano Lett.* 5, 1905–1909
36 Mitsui, T. *et al.* (2006) Nanoscale volcanoes: accretion of matter at ion-sculpted nanopores. *Phys. Rev. Lett.* 96, 036102
37 Lo, C.J. *et al.* (2006) Fabrication of symmetric sub-5 nm nanopores using focused ion and electron beams. *Nanotechnology* 17, 3264–3267
38 Gordon, R.G. *et al.* (2003) A kinetic model for step coverage by atomic layer deposition in narrow holes or trenches. *J. Chem. Vap. Deposition* 9, 73–78
39 Hausmann, D.M. *et al.* (2002) Atomic layer deposition of hafnium and zirconium oxides using metal amide precursors. *Chem. Mater.* 14, 4350–4358
40 Saleh, O.A. and Sohn, L.L. (2003) An artificial nanopore for molecular sensing. *Nano Lett.* 3, 37–38
41 Saleh, O.A. and Sohn, L.L. (2004) Biological sensing with an on-chip resistive pulse analyzer. In *Proceedings of the 26th Annual International Conference of the IEEE EMBS San Francisco, CA, USA*, pp. 2568–2570.
42 Schmid, H. and Michel, B. (2000) Siloxane polymers for high-resolution, high-accuracy soft lithography. *Macromolecules* 33, 3042–3049
43 Mara, A. *et al.* (2004) An asymmetric polymer nanopore for single molecule detection. *Nano Lett.* 4, 497–501
44 Siwy, Z. and Fulinski, A. (2002) Fabrication of a synthetic nanopore ion pump. *Phys. Rev. Lett.* 89, 198103
45 Heins, E.A. *et al.* (2005) Detecting single porphyrin molecules in a conically shaped synthetic nanopore. *Nano Lett.* 5, 1824–1829
46 Harrell, C.C. *et al.* (2003) Synthetic single-nanopore and nanotube membranes. *Anal. Chem.* 75, 6861–6867

47 Harrell, C.C. *et al.* (2004) DNA nanotube artificial ion channels. *J. Am. Chem. Soc.* 126, 15646–15647
48 Storm, A.J. *et al.* (2003) Fabrication of solid-state nanopores with single-nanometre precision. *Nat. Mater.* 2, 537–541
49 Keyser, U.F. *et al.* (2005) Nanopore tomography of a laser focus. *Nano Lett.* 5, 2253–2256
50 Smeets, R.M. *et al.* (2006) Salt dependence of ion transport and DNA translocation through solid-state nanopores. *Nano Lett.* 6, 89–95
51 Heng, J.B. *et al.* (2006) The electromechanics of DNA in a synthetic nanopore. *Biophys. J.* 90, 1098–1106
52 Ho, C. *et al.* (2005) Electrolytic transport through a synthetic nanometer-diameter pore. *Proc. Natl. Acad. Sci. U.S.A.* 102, 10445–10450
53 Chang, H. *et al.* (2004) DNA-mediated fluctuations in ionic current through silicon oxide nanopore channels. *Nano Lett.* 4, 1551–1556
54 Chang, H. *et al.* (2006) Fabrication and characterization of solid-state nanopores using a field emission scanning electron microscope. *Appl. Phys. Lett.* 88, 103109
55 Wu, M. *et al.* (2005) Formation of nanopores in a SiN/SiO_2 membrane with an electron beam. *Appl. Phys. Lett.* 87, 113106
56 Storm, A.J. *et al.* (2005) Electron-beam-induced deformations of SiO_2 nanostructures. *J. Appl. Phys.* 98, 014307
57 Ito, T. *et al.* (2004) A carbon nanotube-based coulter nanoparticle counter. *Acc. Chem. Res.* 37, 937–945
58 Ito, T. *et al.* (2003) Observation of DNA transport through a single carbon nanotube channel using fluorescence microscopy. *Chem. Commun.* 12, 1482–1483
59 Henriquez, R.R. *et al.* (2004) The resurgence of Coulter counting for analyzing nanoscale objects. *Analyst* 129, 478–482
60 Fan, S. *et al.* (1999) Self-oriented regular arrays of carbon nanotubes and their field emission properties. *Science* 283, 512–514
61 Sun, L. and Crooks, R.M. (2000) Single carbon nanotube membranes: a well-defined model for studying mass transport through nanoporous materials. *J. Am. Chem. Soc.* 122, 12340–12345
62 Fan, R. *et al.* (2005) DNA translocation in inorganic nanotubes. *Nano Lett.* 5, 1633–1637
63 Burns, M.A. *et al.* (1998) An integrated nanoliter DNA analysis device. *Science* 282, 484–487
64 Meller, A. *et al.* (2000) Rapid nanopore discrimination between single polynucleotide molecules. *Proc. Natl. Acad. Sci. U. S. A.* 97, 1079–1084
65 Wang, H. *et al.* (2004) DNA heterogeneity and phosphorylation unveiled by single-molecule electrophoresis. *Proc. Natl. Acad. Sci. U. S. A.* 101, 13472–13477
66 Vercoutere, W. *et al.* (2001) Rapid discrimination among individual DNA hairpin molecules at single-nucleotide resolution using an ion channel. *Nat. Biotechnol.* 19, 248–252
67 Howorka, S. *et al.* (2001) Sequence-specific detection of individual DNA strands using engineered nanopores. *Nat. Biotechnol.* 19, 636–639
68 Kasianowicz, J.J. (2004) Nanopores: flossing with DNA. *Nat. Mater.* 3, 355–356
69 Sanchez-Quesada, J. *et al.* (2004) DNA rotaxanes of a transmembrane pore protein. *Angew. Chem. Int. Ed.* 43, 3063–3067
70 Astier, Y. *et al.* (2006) Toward single-molecule DNA sequencing: direct identification of ribonucleoside and deoxyribonucleoside 5′-monophosphates by using an engineered protein nanopore equipped with a molecular adapter. *J. Am. Chem. Soc.* 128, 1705–1710
71 Chang, H. *et al.* (2006) DNA counter ion current and saturation examined by a MEMS-based solid state nanopore sensor. *Biomed. Microdevices* 8, 263–269